Cooperative principle in multiple glass transitions and strain relaxations of thermochemically responsive shape memory polymer

Xiaodong Wang[1], Haibao Lu[1,6], Nan Wu[2], David Hui[3], Mingji Chen[4] and Yong-Qing Fu[5]

[1]Science and Technology on Advanced Composites in Special Environments Laboratory, Harbin Institute of Technology, Harbin 150080, China

[2]Department of Mechanical Engineering, University of Manitoba, Winnipeg, Manitoba, R3T 2N2, Canada

[3]Composite Material Research Laboratory, Department of Mechanical Engineering, University of New Orleans, LA 70148, USA

[4]Institute of Advanced Structure Technology, Beijing Institute of Technology, 100081, Beijing, China

[5]Faculty of Engineering and Environment, University of Northumbria, Newcastle upon Tyne, NE1 8ST, UK

[6]luhb@hit.edu.cn

Abstract: Cooperative principle in shape memory polymers (SMPs) result in their effective communication with the external thermochemical stimuli and then the SMPs act cooperatively to generate stimulus-responsive shape memory effect (SME). Their SME can be triggered by chemical stimuli and the corresponding thermochemically responsive behaviors are often explained by the reversible rearrangement of macromolecule segments due to changes of their configurational entropy. In this paper, we propose a new cooperative model to describe the multiple glass transitions

and strain relaxations of an SMP in response to the water by means of selective and chemical plasticization effect on the partial segments in a macromolecule. Based on this model, the plasticization effect on the glass transition temperature, relaxation time and recovery strain of the SMP have been systematically investigated. Finally, the constitutive model for thermochemically responsive SMPs with two viscoelastic transitions and multiple SMEs was established to describe their overall mechanical responses, and a good agreement between the numerical and experimental results has been achieved.

Keywords: shape memory polymer; viscoelastic transition; relaxation; cooperative

1. Introduction

Shape memory polymers (SMPs) are one type of smart materials which after pre-deformation could recover to their original shapes when exposed to external stimuli, such as heat, light, electricity, magnetic field or chemicals etc. [1-3]. SMPs have their unique shape memory effect (SME) which is originated from their inherently structured features, in which one of the components is the hard segment/phase to determine the permanent shape, and the other one is the soft segment/phase in response to the external stimuli [4,5]. Among all different types of SMPs, thermally activated amorphous SMPs are the most investigated ones because of their wide variety, simplicity in synthesis, widely available characterization methods and constitutive models [6-8]. Taking for example, Liu et.al proposed a useful viscoelastic model for SMP according to the phase transition, and it well

predicted the thermomechanical and time-dependent shape recovery behaviors [9-11]. Meanwhile, Li et.al formulated a thermomechanical constitutive model for the SMP including continuum functional and mechanical damage effect, and it well fits to the experimental results of the nonlinear stress-strain behavior [12].

In recent years, thermochemically responsive SMPs have attracted much more interests owing to their great potentials of applications in biomedicine [13-16]. The self-tightened and biodegradable water-driven SMP stents and scaffolds [15,17] have now been developed to meet the stringent requirements in the minimally invasive surgery, and their degradation rates can be purposely designed and adjusted in water [17]. Furthermore, multi-functions [18,19] and multi-SMEs [20-22] in these SMPs are expected to significantly expand their practical applications. To model the water-driven SME, Xiao et. al [23] formulated a constitutive model for the thermomechanical properties and shape-memory performance of amorphous polymers using the configurational entropy parameters. Yu et. al [24,25] proposed a viscoelastic model for the hydrothermally activated covalent network polymer. In our previous studies [26-28], the athermal recovery behavior and permeation transition processes have been systematically studied based on polymer physics. However, so far, there are no good constitutive models available to describe the cooperative mechanisms for the thermochemically responsive SMPs with multiple phase transitions and multi-SMEs.

The general design methodology of these thermochemically responsive SMP is based on the utilizations of plasticizing effect to decrease the glass transition temperature (T_g), and then trigger their phase transition and SME at room temperature

by means of releasing the stored mechanical energy in the polymer macromolecules [29,30]. Experimental studies revealed that the absorbed water molecules have a strong plasticizing effect on the soft segments by forming hydrogen bonds [31]. The plasticizing effect has been identified as the key driving force to enhance the mobility of the macromolecules by significantly decreasing their activation energy barriers, and thus resulting in decreases of both the thermomechanical storage modulus and T_g, which have been verified by the dynamic mechanical analysis (DMA) [29]. On the other hand, the physical swelling effect generated along with the SME has also influence the T_g [31].

To further explore and fully understand the working mechanisms of the thermochemically induced viscoelastic transition and SME in the SMPs, the effects of free water and bound water on the viscoelastic transition and recovery strain have firstly been discussed in this study separately. The effect of bound water on the T_g of soft segment is then modelled according to the Gordon-Taylor equation [32]. Based on the Vogel-Tamman-Fulcher (VTF) equation [33], the viscoelastic storage modulus and relaxation behavior are investigated and the simulation results are compared with the experimental data reported in Ref. [29,31,34] for verification. To extend the application of the proposed model, theoretical analysis is finally performed on the thermochemically induced multiple glass transitions and strain relaxations in the SMP.

2. Modelling of thermochemically induced viscoelastic transition

2. 1 Effect of bound water on T_g

Polyurethane SMP is composed of both hard and soft segments (or phases). The

plasticizing effect of the bound water has been identified as the driving force for the thermochemically induced SME by means of the hydrogen bonding between the bound water and soft segment. Effect of the weight fraction of the absorbed bound water (w_m) on the T_g of soft phase ($T_g(s)$) can be expressed as [35,36]:

$$T_g(s) = (T_{g0} - T_{gl}) \exp\left[-\ln(T_{g0} - T_{gl}) w_m / (w_{ml} - \delta) \right] + T_{gl} \quad (1)$$

where T_{g0} is the glass transition temperature of soft segment, and w_m =0, T_{gl} is the lowest value of T_g caused by the plasticizing effect, and the corresponding weight fraction of water is w_{ml}. The term $(w_{ml} - \delta)$ indicates the conjugate value for the weight fraction of water at $T_g(s) = T_{gl} + 1$. Equation (1) can be used to characterize the plasticizing effect of bound water on the soft segment. However, the hard segment also plays an essential role to determine the T_g of the polymer. Therefore the effects of glass transition temperatures ($T_g(h)$ and $T_g(s)$) of both the soft and hard segments on the T_g of the polymer can be expressed by [37]:

$$T_g = \phi_s T_g(s) + \phi_h T_g(h) \quad (2)$$

where $T_g(h)$ is assumed to be a constant value because the plasticizing effect has insignificant effect on it, and ϕ_s and ϕ_h are the volume fractions of the soft and hard segments, respectively .

Equation (2) can be rewritten according to the Gordon-Taylor equation [32]:

$$T_g = \left[w_s T_g(s) + K w_h T_g(h) \right] / (w_s + K w_h) \quad (3)$$

where w_s and w_h are the weight fractions of soft and hard segments, respectively, and K is a constant.

When the weight fraction of water is w_m, then w_s and w_h can be expressed as

follows:

$$\begin{cases} w_s = (1-w_m)w_s^{'} + w_m \\ w_h = (1-w_m)w_h^{'} \end{cases} \tag{4}$$

where $w_s^{'}$ and $w_h^{'}$ are the weight fractions of soft and hard segments, respectively, without absorbing the water molecules.

By substituting equations (1) and (4) into equation (3), we can obtain the following expression:

$$\begin{aligned} T_g = \{&\left[(1-w_m)w_s^{'} + w_m\right]\cdot\left[(T_{g0}-T_{gl})\exp(-\ln(T_{g0}-T_{gl})w_m/(w_{ml}-\delta)) + T_{gl}\right] \\ &+ K(1-w_m)w_h^{'}T_g(h)\}/\left[(1-w_m)w_s^{'} + w_m + K(1-w_m)w_h^{'}\right] \end{aligned} \tag{5}$$

Figure 1 plots the simulation results obtained from the equation (5) and the experimental data of the water-driven polyurethane SMP [29] for comparisons. Values of the parameters used in equation (5) have been summarized in Table 1, where the parameters are determined by the Universal Global Optimization (UGO) algorithm. It is found that the simulation results from the proposed model are in a good agreement with the experimental data. The decrease rate of T_g is quite significant initially, but then it is gradually reduced with a further increase in the weight fraction of the bound water. With an increase in the weight fraction of the bound water from 0% to 3.6%, the T_g is decreased from 309 *K* to 281.9 *K*. When the T_g value is 281.9 *K* which reaches to the ambient temperature, the SME is then triggered without additionally thermal heating. Being different from the thermally induced SME, the water-driven one is mainly resulted from the hydrogen bonding between the polymer and bound water by inductively decreasing the T_g of soft segment [31].

[Table 1]

[Figure 1]

To achieve the chemical actuation of SME, the $T_g(h)$ and $w_h^{'}$ are two important parameters which will determine the decrease in T_g of the SMPs according to equation (5). Figure 2 presents the constitutive relationship for the T_g of the SMP as a function of weight fraction of bound water at various fixed weight fraction ($w_h^{'}$) and glass transition temperatures ($T_g(h)$) of hard segments, e.g., $w_h^{'} = 0\%$, 5%, 10%, 15% and 20%, and $T_g(h) = 340\ K$, 345 K, 350 K, 355 K and 360 K. As shown in Figure 2(a), the $w_h^{'}$ plays an essential role to determine the T_g of the SMP as a function of the weight fraction of bound water. By decreasing the weight fraction of the hard segment from 20% to 0%, the decrease in the T_g of the SMP becomes significant, mainly because the absorbed water has insignificant effect on the hard segment. On the other hand, the T_g values of the SMP is gradually decreased with a decrease in the $T_g(h)$. For the SMP with a lower value of $T_g(h)$, the T_g of the SMP is therefore decreased according to the equations (2) or (3), as shown in Figure 2(b).

[Figure 2]

As most of polymers has certain amount of voids, the absorbed water in the SMP can be divided into two different types, namely the bound water and free water. The bound water is absorbed into the polymer network and therefore has a plasticizing effect on the polymer macromolecules, whereas the free water only occupies the space of voids, without any chemical interaction with the macromolecules.

According to the free-volume theory [38,39] and quasi-lattice theory [40], the volume of the amorphous polymers is treated as two parts: one is occupied by the

macromolecules, and the other is unoccupied free volume existed in the polymer systems as the void to allow the mobility of macromolecule chains. When immersed into the water, the free water occupies the position of void and the free volume (f) of void in polymer can be expressed as [38]:

$$f = f_g + \alpha_f (T - T_g) \tag{6}$$

where α_f is the coefficient thermal expansion of void and f_g is the fractional volume of the void in polymer at T_g. Equation (6) can also be re-written using the weight fraction. The volume fraction of the free water (f) and weight fraction of the free water (w_f) can be expressed as:

$$f = \frac{V_f}{V_f + V_p}; \quad w_f = \frac{V_f \rho_f}{V_f \rho_f + V_p \rho_p} \tag{7}$$

where V_f and V_p are the volumes of free water and polymer combined with bound water, respectively. Parameters ρ_f and ρ_p are their corresponding densities, respectively. Equation (7) could be also re-written as follows:

$$\frac{V_p}{V_f} = \frac{1}{f} - 1; \quad w_f = 1 / \left(1 + \frac{V_p}{V_f} \cdot \frac{\rho_p}{\rho_f} \right) \tag{8}$$

Therefore, we can obtain:

$$w_f = 1 / \left(1 + \left(\frac{1}{f} - 1 \right) \cdot \frac{\rho_p}{\rho_f} \right) \tag{9}$$

Based on the assumption that the density of the polymer is approximately equal to the density of the water, i.e. $\rho_p = \rho_f$, we can get:

$$w_f = f = f_g + \alpha_f (T - T_g) \tag{10}$$

where w_f and w_g are the weight fractions of the free water at the temperature of T and T_g, respectively.

By substituting equation (5) into (10), we can obtain the equation of the weight fraction of free water as functions of the glass transition temperatures and weight fraction of the bound water (w_m):

$$w_f = w_g + \alpha_f \begin{Bmatrix} T - \{\left[(T_{g0} - T_{gl})\exp(-\ln(T_{g0} - T_{gl})w_m / (w_{ml} - \delta)) + T_{gl}\right] \cdot \left[(1 - w_m)w_s^{'} + w_m\right] \\ + K(1 - w_m)w_h^{'}T_g(h)\} / \left[(1 - w_m)w_s^{'} + w_m + K(1 - w_m)w_h^{'}\right] \end{Bmatrix} \quad (11)$$

The overall weight fraction of water (w) is incorporated from both the bound and free water and can be therefore expressed:

$$w = w_m + w_f \quad (12)$$

In order to verify the accuracy of equations (5) and (11), a comparison was performed between the simulation results using these two equations and the reported experimental ones from Ref. [29]. The constants used in the comparison for the equation (11) are listed in Table 1, while the parameters $w_g = 1.3\%$ and $\alpha_f = 0.0007(1/K)$ have also been used. Figure 3 plots the numerical results of the T_g of the SMP as a function of the weight fraction of water ($w = w_m + w_f$), and the experimental data from Ref. [29] are also plotted inside for comparisons, where the immersion times are 2 hours, 12 hours and 48 hours. Simulation results reveal that the T_g decreases gradually with an increase in the weight fraction of water, and are in good agreements with the experimental ones. Results show that the bound water has apparent effects on the T_g of the SMP. Although both bound water and free water have been absorbed into the polymer, whereas the free water is only absorbed and has the key effects on the permeability of the polymers [39].

[Figure 3]

2.2 Effect of bound water on relaxation time

As discussed above, the significant decrease of the T_g of the SMP is mainly due to the bound water inside. Therefore, it is necessary to characterize the effect of bound water on the viscoelastic relaxation behavior which is determined by not only the glass transition, but also the relaxation time of the SMP. According to Vogel-Tamman-Fulcher (VTF) equation [33,40], the temperature dependence of relaxation time can be written as:

$$\tau = A\exp(B/(T-T_0)) \tag{13}$$

where A and B are the material constants, T_0 is a thermodynamic parameter of temperature at which the relaxation time is infinite [41].

Based on the experimental results [41], the values of T_g and T_0 have the following relationship:

$$T^* - T_0 + T_g = 550K \tag{14}$$

where T^* is the temperature limit of the segments which are sufficiently separated apart from each other and relaxed independently. For example, the value of T^* is 773 K for all types of polymers [41].

By integrating equations (5) and (14) into equation (13), we can obtain the relationship between the weight fraction of the bound water (w_m) and the relaxation time (τ):

$$\tau = A\exp\left\{\begin{array}{l} B/\{T-T^*-\{\left[(1-w_m)w_s^{'}+w_m\right]\cdot \\ \left[(T_{g0}-T_{gl})\exp(-\ln(T_{g0}-T_{gl})w_m/(w_{ml}-\delta))+T_{gl}\right] \\ +K(1-w_m)w_h^{'}T_g(h)\}/\left[(1-w_m)w_s^{'}+w_m+K(1-w_m)w_h^{'}\right]+550\} \end{array}\right. \tag{15}$$

The calculated results of the effect of the w_m on the relaxation time of SMP are

plotted in Figure 4. The constants used in the equation (15) are listed in Table 2, where the parameters are also determined by the UGO algorithm as mentioned above. It is found that the relaxation time is significantly decreased with an increase in the weight fraction of the bound water until the glass transition temperature (T_g) reaches T_{gl}. These simulation results confirm the plasticizing effect of the bound water on the T_g, which has also indirectly lowered the T_0 of the SMP according to the equation (14). The relaxation time is decreased with a decrease in the T_0 based on the equation (15). Therefore, the relaxation time is indirectly decreased with the increase in the w_m.

The relaxation time is also determined by the weight fraction of the soft segment. As the weight fraction of the soft segment is decreased from w_s'=100%, 95%, 90% down to 85% in the SMP, the relaxation time is gradually increased from τ=1.85 s, 3.51 s, 5.02 s to 6.28 s with a fixed bound water of w_m=2.5%. With the increase in the weight fraction of the soft segment, the T_g of the SMP is decreased according to equations (2) and (3), which also results in a decrease of the T_0 based on the equation (14). Therefore the working mechanisms behind the effects of both the w_m and w_s' parameters on the relaxation time are similar to each other.

[Figure 4]

2.3 Effect of bound water on the storage modulus

To verify the theoretical models for the predictions of storage modulus of the SMP, the experimental data of the storage moduli measured using a dynamic mechanical analyzer (DMA) have been used to compare with the simulation ones. The absorbed

bound water has been found to decrease the glass transition temperature and relaxation time, both of which are critical for the viscoelastic properties of the SMP, including the essential parameter of storage modulus.

The decrease of the storage modulus ($E(s)$) of the soft segment can be described as follows [35,36]:

$$E(s) = (\Delta E_0) \exp\left\{-\left[\ln(\Delta E_0)\right] w_m / \upsilon w_{ml}\right\} + E_l \tag{16}$$

where $\Delta E_0 = E_0 - E_l$, E_0 and E_l are the storage moduli of the polymer when the weight fraction of the soft segment are $w_m = 0$ and $w_m = w_{ml}$, respectively, and υ is a given constant.

The storage modulus (E) of the SMP can therefore be obtained according to the Gordon-Taylor equation [32]:

$$E = [w_s E(s) + K w_h E(h)] / (w_s + K w_h) \tag{17}$$

where $E(h)$ is the storage modulus of the hard segment.

By substituting equations (4) and (16) into equation (17), we can obtain:

$$\begin{aligned} E = \{&\left[(1-w_m) w_s^{'} + w_m\right] \cdot \left[(\Delta E)_0 \exp\left\{-\left[\ln(\Delta E)_0\right] w_m / \upsilon w_{ml}\right\} + E_l\right] \\ &+ K(1-w_m) w_h^{'} E(h)\} / \left[(1-w_m) w_s^{'} + w_m + K(1-w_m) w_h^{'}\right] \end{aligned} \tag{18}$$

To verify the equation (18), the calculated results have been plotted in Figure 5, while the experimental data [34] obtained from the styrene-based SMP have also been presented for a comparison. The SMP was immersed in the N,N-Dimethylformamide (DMF) solvent for different durations of 10 min, 30 min, 60 min and 120 min, respectively. All the parameters used in the calculation are listed in Table 2. It is found that the simulation results are in good agreements with the experimental ones. With an increase in the immersion time from 10 min to 120 min, the storage modulus of the

SMP is decreased from 1196 MPa to 604 MPa. Generally, the plasticizing effect of solvent molecules on the SMP significantly reduces the intermolecular forces among the polymer macromolecules [34]. Therefore, the storage modulus is decreased accordingly due to the plasticizing effect which is identified as the key working mechanism of the thermochemically induced SME in SMP.

[Table 2]

[Figure 5]

3. Modelling of the thermochemically induced shape recovery behavior

Based on the equation (1), the bound water has a significant influence on the decrease in the glass transition temperature of the soft segment in polyurethane SMP. Here, it is necessary to study the effect of the bound water on the shape recovery behavior which is always used to characterize the SME in SMPs. According to the phase transition theory [42], the relationship between recovery strain (ε) and temperature (T) of the SMP can be written by the following equation:

$$\varepsilon = \varepsilon_{pre}\left(1-\frac{1}{1+c_f(T_h-T)^n}\right) \tag{19}$$

where ε_{pre} is the pre-loading strain, c_f and n are given constants. T_h is the phase transition temperature, which is different from the glass transition temperature according to the following equation:

$$T_h = T_g + k \tag{20}$$

where k is the difference between T_h and T_g.

By substituting equations (1) and (20) into (19), we can obtain the constitutive relationship between the recovery strain (ε) and weight fraction of bound water (w_m)

in the SMP using the following equation:

$$\varepsilon = \varepsilon_{pre}\left(1-\frac{1}{1+c_f\{(T_{g0}-T_{gl})\exp\left[-\ln(T_{g0}-T_{gl})w_m/(w_{ml}-\delta)\right]+T_{gl}+k-T\}^n}\right) \quad (21)$$

Meanwhile, the recovery stress (σ) can be determined by the recovery strain (1-ε) and modulus (E), we have:

$$\sigma=(1-\varepsilon)\cdot E \quad (22)$$

Based on the Fick's second law, Crank and Park [43] have suggested the following simplified relationship for the weight fraction of water (w_m) with respect to time t:

$$w_m(t) \cong \frac{4}{b\sqrt{\pi}}\sqrt{D}\sqrt{t} \quad (23)$$

where D is the diffusion coefficient and b is a given constant.

To further verify the proposed model, the experimental data of recovery strain and stress of the ether-based polyurethane SMP [31] have been employed. The values of parameters are summarized in Table 3. It is found that both recovery strain and stress are increased with an increase in the immersion time. The recovery strain reaches to the maximum value of 54% when the tested SMP is immersed into water for 8 hours. On the other hand, the stress reaches to the maximum value 0.38 MPa when the immersion time is 4.6 hours. A good agreement between the numerical with experimental results has been found for the recovery strain and stress as a function of immersion time.

[Table 3]

[Figure 6]

Based on the experimental results reported in Ref. [44], each soft segment has its

own initial glass transition temperature (T_{g0}) in SMP which is incorporated from one hard segment and multiple soft segments. Based on the Boltzmann's superposition principle, we can rewrite equation (21) for the recovery strain of the SMP with multiple soft segments using the following equation:

$$\varepsilon = \sum_{i=1}^{\beta} \varepsilon_{pre}(i)\left(1 - \frac{1}{1 + c_f(i)\{(\Delta T_g(i))\exp\left[-\ln(\Delta T_g(i))w_m/(w_{ml}-\delta)_i\right] + T_{gl}(i) + k - T\}^{n(i)}}\right) \quad (24)$$

where $\varepsilon_{pre}(i)$, $c_f(i)$, $\Delta T_g(i)$, $(w_{ml}-\delta)_i$, $T_{gl}(i)$ and $n(i)$ are the corresponding parameters for the *i*th soft segment, and β is the number of soft segments. When $T_g(i)+k-T=0$ for the *i*th soft segment, it is assumed that the recovery strain for the *i*th segment is completely achieved and regains its original state. According to previous work [42], values of the parameters used in Equation (24) have been given as, $c_f = 2.76\times10^{-5}$, $n=4$, $T=293K$, $T_{gl}=285.5K$ and $\varepsilon_{pre}=0.5$.

The simulation results of the SMP with two soft segments have been plotted in Figure 7. The effect of the glass transition temperature of the second soft segment ($T_{g0}(2)$) on the recovery strain has been studied and the simulation results are plotted in Figure 7(a). It is revealed that the recovery strain is gradually increased with an increase of the $T_{g0}(2)$. At a given $T_{g0}(1)$ =340 *K*, the recovery strain is gradually increased with the increase in the $T_{g0}(2)$ from 360 *K*, 400 *K*, 440 *K*, 480 *K* to 520 *K*. That is to say, the two-stage transition becomes more significant when the difference in the glass transition temperatures of the two soft segments is becoming larger.

On the other hand, the effect of the weight fraction of the bound water absorbed by the second soft segment ($(w_{ml}-\delta)_2$) on the recovery strain has also been investigated and the simulation results are plotted in Figure 7(b). At the fixed values of $T_{g0}(1)$

=340 K and $T_{g0}(2)$ =380 K, the recovery strain is gradually increased with the increase in the values of $(w_{ml}-\delta)_2$ from 6%, 8%, 10%, 12% up to 14%. That is to say, the two-stage transition becomes more apparent with the increase in the difference in the weight fraction of the bound water absorbed by the second soft segment. These simulation results reveal that the two-stage recovery strain is determined not only by the intrinsic differences in the glass transition temperatures of the two soft segments, but also by the weight fraction of the bound water. This indicates that there are two effective approaches which can be used to design the two-stage shape recovery behavior, e.g., either by control of the difference in the glass transition temperatures, or by control of the plasticizing effect due to the weight fraction of the bound water on the soft segments.

[Figure 7]

Furthermore, we can use the proposed model to predict the multiple glass transitions and strain relaxations by changing the T_{gl} through the plasticizing effect. Figure 8 plots the numerical results of the recovery strain as a function of weight fraction of the bound water, when the following parameters are fixed, e.g., $T_{g0}(1)$ =340 K, $T_{g0}(2)$ =360 K, $(w_{ml}-\delta)_1=(w_{ml}-\delta)_2$ =10% and $T_{gl}(2)$ =300K (295K, 290K, 285K or 280K). It is found that the $T_{gl}(2)$ has a significant influence on the recovery strain. With an increase in the $T_{gl}(2)$, the decrease in recovery strain curve becomes less significant. Simulation results also confirm that the recovery strain is gradually increased with an increase in the temperature of $T_{gl}(2)$ due to a large difference in the glass transition temperatures of the two soft segments.

[Figure 8]

In order to further explore the working mechanism and provide an effective theoretical approach to design the thermochemically driven multi-SME and multiple shape recovery behavior, Figure 9 plots the constitutive relationship of the glass transition temperature and weight fraction of bound water for the SMP which is incorporated from multiple soft segments. As revealed in Figure 9(a), the T_g is gradually increased with the increase in the difference of the weight fraction of bound water in the second soft segment $(w_{ml}-\delta)_2$ from 6%, 8%, 10%, 12% to 14%, when $(w_{ml}-\delta)_1$=4%, $T_{g0}(1)$=340 K and $T_{g0}(2)$=380 K. These simulation results show the significant effect of bound water on the thermomechanical properties. According to equation (15), the decrease in storage modulus becomes insignificant with an increase in the weight fraction of the bound water ($(w_{ml}-\delta)_2$). On the other hand, the simulation results for the effect of glass transition temperature of the second soft segment ($T_{gl}(2)$) on the SMP are summarized in Figure 9(b), which can explain the changes of the thermomechanical transition of the polymer. These simulation results confirm that the $T_{gl}(2)$ has a significant effect on the T_g of the SMP.

[Figure 9]

The simulation and experimental results reveal that the working mechanism behind thermochemically induced multiple SME and strain relaxations is resulted from the decrease in the transition temperature of the SMPs, instead of thermal heating. However, the thermally and thermochemically induced SMEs can both be described using the Arrhenius equation [34]. Therefore, it is necessary to further investigate the

synergistic effect of the thermal and chemical stimuli on the SMP. Here a two-stage shape recovery process was characterized for the SMP which is incorporated of a hard segment and a soft one, with the latter's glass transition temperature is changing from $T_{gl} = 296\ K$, 298 K, 300 K, 302 K to 304 K.

In the first recovery stage, the shape recovery of the SMPs is induced by the water, and the recovery strain curves reveal a decrease in recovery strain as a function of the weight fraction of the water. Consequently, the SMPs are thermally heated after they are removed from the water at the second recovery stage. The recovery strain of the SMPs is thermally induced in this process. An artificial two-stage shape recovery has been achieved for the SMPs using the synergistic effect of the thermal and thermochemical stimuli, as shown in Figure 10.

[Figure 10]

4. Conclusion

In this study, a cooperative model was formulated to describe the unique characteristics of thermochemically multiple glass transitions and strain relaxations in the SMP. Both the thermomechanical properties and shape recovery behavior of the SMP have been simulated using the proposed model, and the simulation results are further compared with the experimental ones for validation. The constitutive relationships among glass transition temperature, storage modulus of the SMPs and weight fraction of bound water have been systematically investigated. The model is then applied to simulate the two glass transitions and strain relaxations in the SMPs with one hard and two soft segments. The obtained results have demonstrated that the

model can successfully describe the multiple glass transitions and strain relaxations. From the numerical analysis of our proposed model, a design principle which is favorable to trigger the multiple SMEs by means of the synergistic effect of thermal and thermochemical stimuli is proposed and discussed. This study is expected to provide a powerful tool to understand the cooperative principle and provide an effectively theoretical guidance for the design of multiple SMEs through thermochemically induced glass transitions and strain relaxations in SMPs.

Acknowledgements

This work was financially supported by the National Natural Science Foundation of China (NSFC) under Grant No. 11672342 and 11725208, Newton Mobility Grant (IE161019) through Royal Society and NFSC.

Reference

[1] Razzaq M Y, Anhalt M, Frormann L and Weidenfeller B 2007 Thermal, electrical and magnetic studies of magnetite filled polyurethane shape memory polymers *Mater. Sci. Eng. A* **444** 227-35

[2] Beblo R V and Weiland L M 2009 Light activated shape memory polymer characterization *J. Appl. Mech.* **76** 011008

[3] Mendez J, Annamalai P K, Eichhorn S J, Rusli R, Rowan S J, Foster E J and Weder C 2011 Bioinspired mechanically adaptive polymer nanocomposites with water-activated shape-memory effect *Macromolecules* **44** 6827-35

[4] Gilormini P and Diani J 2012 On modeling shape memory polymers as thermoelastic two-phase composite materials *C. R. Mecanique* **340** 338-48

[5] Tian M and Venkatesh T A 2013 Indentation of shape memory polymers: Characterization of thermomechanical and shape recovery properties *Polymer* **54** 1405-14

[6] Diorio A M, Luo X, Lee K M and Mather P T 2011 A functionally graded shape memory polymer *Soft Matter* **7** 68-74

[7] Wang Y, Li Y, Luo Y, Huang M and Liang Z 2009 Synthesis and characterization of a novel biodegradable thermoplastic shape memory polymer *Mater. Lett.* **63** 347-9

[8] Lu H, Wang X, Yao Y and Fu Y 2018 A 'frozen volume' transition model and working mechanism for the shape memory effect in amorphous polymers *Smart Mater. Struct.* **27** 065023

[9] Li Y, Hu J and Liu Z 2017 A constitutive model of shape memory polymers based on glass transition and the concept of frozen strain release rate *Int. J. Solids Struct.* **124** 252-63

[10] Li Y and Liu Z 2018 A novel constitutive model of shape memory polymers combining phase transition and viscoelasticity *Polymer* **143** 298-308

[11] Pan Z, Zhou Y, Zhang N and Liu Z 2018 A modified phase-based constitutive model for shape memory polymers *Polym. Int.* **67** 1677-83

[12] Shojaei A and Li G 2014 Thermomechanical constitutive modelling of shape memory polymer including continuum functional and mechanical damage effects *Proc. R. Soc. A Math. Phys. Eng. Sci.* **470** 2170

[13] Guo Y, Lv Z, Huo Y, Sun L, Chen S, Liu Z, He C, Bi X, Fan X and You Z 2019 A biodegradable functional water-responsive shape memory polymer for biomedical *J. Mater. Chem. B.* **7** 123-32

[14] Song J, Chang H and Naguib H 2015 Biocompatible shape memory polymer actuators with high force capabilities *Eur. Polym. J.* **67** 186-198

[15] Xie Y, Lei D, Wang S, Liu Z, Sun L, Zhang J, Qing F, He C and You Z 2019 A biocompatible, biodegradable and functionalizable copolyester and its application in water-responsive shape memory scaffold *Acs. Biomater. Sci. Eng.* **5** 1668-1676

[16] Sonawane V C, More M P, Pandey A P, Patil P O and Deshmukh P K 2017 Fabrication and characterization of shape memory polymers based bioabsorbable biomedical drug eluting stent *Artif. Cell. Nanomed. B.* **45**

1740-50

[17] Kelch S, Steuer S, Schmidt A M and Lendlein A 2007 Shape-memory polymer networks from oligo[(ε-hydroxycaproate)-co-glycolate]dimethacrylates and butyl acrylate with adjustable hydrolytic degradation rate *Biomacromolecules* **8** 1018-27

[18] Gunes I S and Jana S C 2008 Shape memory polymers and their nanocomposites: a review of science and technology of new multifunctional materials *J. Nanosci. Nanotechnol.* **8** 1616-27

[19] Ren H, Mei Z, Chen S, Zhuo H, Chen S, Yang H, Zuo J and Ge Z 2016 *J. Mater. Sci.* **51** 9131-44

[20] Carrell J, Zhang H C, Wang S and Tate D 2013 Shape memory polymer nanocomposites for application of multiple-field active disassembly: experiment and simulation *Environ. Sci. Technol.* **47** 13053-59

[21] Wang X, Lu H, Shi X, Yu K and Fu Y 2019 A thermomechanical model of multi-shape memory effect for amorphous polymer with tunable segment compositions *Compos. Part B Eng.* **160** 298-305

[22] Xie T 2011 Recent advances in polymer shape memory *Polymer* **52** 4985-5000

[23] Xiao R and Nguyen T D 2013 Modeling the solvent-induced shape-memory behavior of glassy polymers *Soft Matter* **9** 9455-64

[24] Mao Y, Chen F, Hou S, Qi H and Yu K 2019 A Viscoelastic Model for Hydrothermally Activated Malleable Covalent Network Polymer and its Application in Shape Memory Analysis *J. Mech. Phys. Solids* **18** 31141-4

[25] Luo C, Lei Z, Mao Y, Shi X, Zhang W and Yu K 2018 Chemomechanics in the

Moisture-Induced Malleability of Polyimine-Based Covalent Adaptable Networks *Macromolecules* **51** 9825-38

[26] Lu H, Huang W and Leng J A 2014 phenomenological model for simulating the chemo-responsive shape memory effect in polymers undergoing a permeation transition. *Smart Mater. Struct.* **23** 045038

[27] Lu H and Huang W 2013 A phenomenological model for the chemo-responsive shape memory effect in amorphous polymers undergoing viscoelastic transition *Smart Mater. Struct.* **22** 105019

[28] Lu H and Du S 2014 A phenomenological thermodynamic model for the chemo-responsive shape memory effect in polymers based on Flory–Huggins solution theory *Polymer Chemistry* **5** 1155-1162

[29] Huang W, Yang B, An L, Li C and Chan Y 2005 Water-driven programmable polyurethane shape memory polymer: demonstration and mechanism *Appl. Phys. Lett.* **86** 114105

[30] Huang W, Yang B, Zhao Y and Ding Z 2010 Thermo-moisture responsive polyurethane shape-memory polymer and composites: a review *J. Mater. Chem.* **20** 3367-81

[31] Yang B, Huang W, Li C and Li L 2006 Effects of moisture on the thermomechanical properties of a polyurethane shape memory polymer *Polymer* **47** 1348-56

[32] Gordon M and Taylor J 1952 Ideal copolymers and the second‐order transitions of synthetic rubbers. I. Non‐crystalline copolymers *J. Appl. Chem.* **2** 493-500

[33] Bisquert J, Henn F and Giuntini J C 2005 A simple model of entropy relaxation for explaining effective activation energy behavior below the glass transition temperature *J. Chem. Phys.* **122** 094507

[34] Lv H, Leng J, Liu Y and Du S 2008 Shape−memory polymer in response to solution *Adv. Eng. Mater.* **10**, 592-5

[35] Reimschuessel H K 1978 Relationships on the effect of water on glass transition temperature and young's modulus of nylon 6 *J. Polym. Sci. Polym. Chem.* **16** 1229-36

[36] Hancock B C and Zografi G 1995 Molecular mobility of amorphous pharmaceutical solids below their glass transition temperatures *Pharm. Res.* **12** 799-806

[37] Goldstein M and Nakonecznyi M 1965 Volume relaxation in zinc chloride glass *Phys. Chem. Glasses* **6** 126-131

[38] Lu H, Leng J and Du S 2013 A phenomenological approach for the chemo-responsive shape memory effect in amorphous polymers *Soft Matter* **9** 3851-8

[39] Kovacs A J, Aklonis J J, Hutchinson J M and Ramos A R 1979 Isobaric volume and enthalpy recovery of glasses. II. A transparent multiparameter theory *J. Polym. Sci. Polym. Chem.* **17**, 1079-162

[40] Lu H and Huang W 2013 On the origin of the Vogel-Fulcher-Tammann law in the thermo-responsive shape memory effect of amorphous polymers *Smart Mater. Struct.* **22** 105021

[41] Matsuoka S and Quan X 1991 A model for intermolecular cooperativity in conformational relaxations near the glass transition *Macromolecules* **24** 2770-9

[42] Liu Y, Gall K, Dunn M L, Greenberg A R and Diani J 2006 Thermomechanics of shape memory polymers: uniaxial experiments and constitutive modeling *Int. J. Plast.* **22** 279-313

[43] Crank J and Park G S 1968 Diffusion in polymers *Academic Press, London*

[44] Xie T, Xiao X and Cheng Y 2009 Revealing triple−shape memory effect by polymer bilayers *Macromol. Rapid Commun.* **30** 1823-27

Tables caption

Table 1. Values of parameters used in equation (5).

Table 2. Value of parameters used in equations (5) and (15).

Table 3. Value of parameters used in equations (21) and (22).

Figures caption

Figure 1. Comparisons of the T_g values obtained from simulation results obtained using equation (5) and the experimental data obtained from Ref. [29] as a function of the weight fraction ratio of bound water.

Figure 2. The simulation results of the T_g of the SMP as a function of weight fraction of bound water. (a) $w_h^{'} = 0.20$, 0.15, 0.10, 0.05 and 0. (b) $T_g(h) = 340K$, $345K$, $350K$, $355K$ and $360K$.

Figure 3. Effects of the bound and free water on the T_g of the SMP as a function of weight fraction of water.

Figure 4. Numerical results for the relaxation time as a function of weight fraction of bound water at a given $w_s^{'}$, where $w_s^{'}$=100%, 95%, 90% and 85%.

Figure 5. Comparisons between the simulation results and experimental data [34] of storage modulus and T_g as a function of weight fraction of DMF solvent.

Figure 6. Comparisons between the simulation results and experimental data [31] of the recovery ratio and recovery stress with respect to time.

Figure 7. Simulation results of the recovery strain of the SMP as a function of weight fraction of bound water. (a) Simulation curves for the recovery strain at a glass transition temperature of the second soft segment $T_{g0}(2)$=360 K, 400 K, 440 K, 480 K to 520 K. (b) Simulation curves for the recovery strain at a given weight fraction of the bound water absorbed by the second soft segment $(w_{ml} - \delta)_2$=6%, 8%, 10%, 12% to 14%.

Figure 8. Simulation results of the recovery strain of the SMP as a function of weight

fraction of bound water at a given glass transition temperature of the second soft segment $T_{gl}(2)$ =300K, 295K, 290K, 285K and 280K.

Figure 9. Simulation results of the glass transition temperatures of the SMP as a function of weight fraction of bound water. (a) Simulation curves for the glass transition temperatures at a given $(w_{ml}-\delta)_2$ of the second soft segment $(w_{ml}-\delta)_2$ =6%, 8%, 10%, 12% to 14%. (b) Simulation curves for the glass transition temperatures at a given $T_{gl}(2)$ of the second soft segment $T_{gl}(2)$ =300K, 295K, 290K, 285K and 280K.

Figure 10. Simulation results of the two-stage recovery strain of the SMP as a function of weight fraction of bound water and temperature, respectively.

Table 1.

$T_g(h)(K)$	$T_{gl}(K)$	$T_{g0}(K)$	K	$w_s^{'}$	$w_h^{'}$	$w_{ml}-\delta$ (%)
350	260	297.02	6.18	0.95	0.05	2.35

Table 2.

$w_s^{'}$	$E_l(MPa)$	$E_{\mathrm{h}}(MPa)$	$\Delta E_0(MPa)$	υw_{ml}	$T_{gl}(K)$	$T_{\mathrm{h}}(K)$	$T_{g0}(K)$	$w_{ml}-\delta$
0.5	400	3000	3067	3.99	300	370	378.9	3.0698

Table 3.

$w_s^{'}$	$E_l(MPa)$	$\Delta E_0(MPa)$	K	υw_{ml}	$\frac{4}{\mathrm{b}\sqrt{\pi}}\sqrt{D}$	$T_{gl}(K)$	$T_{\mathrm{h}}(K)$	$T_{g0}(K)$	$w_{ml}-\delta$
0.97	1.385	974.03	12.1	0.021	1.57	270	340	280	0.0137

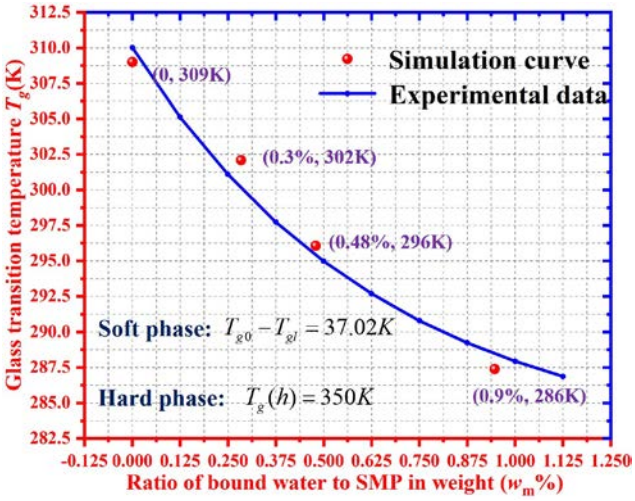
Glass transition temperature T_g(K)
Ratio of bound water to SMP in weight (w_m%)
Simulation curve
Experimental data
(0, 309K)
(0.3%, 302K)
(0.48%, 296K)
(0.9%, 286K)
Soft phase: $T_{g0} - T_{gl} = 37.02K$
Hard phase: $T_g(h) = 350K$

Figure 1.

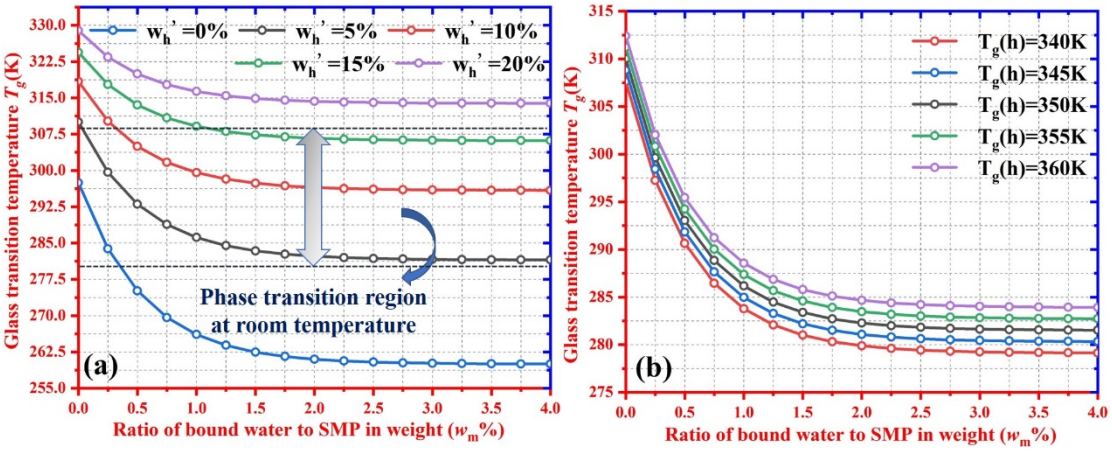
Glass transition temperature T_g(K)
w_h' =0%
w_h' =5%
w_h' =10%
w_h' =15%
w_h' =20%
Phase transition region
at room temperature
(a)
Ratio of bound water to SMP in weight (w_m%)
Glass transition temperature T_g(K)
T_g(h)=340K
T_g(h)=345K
T_g(h)=350K
T_g(h)=355K
T_g(h)=360K
(b)
Ratio of bound water to SMP in weight (w_m%)

Figure 2.

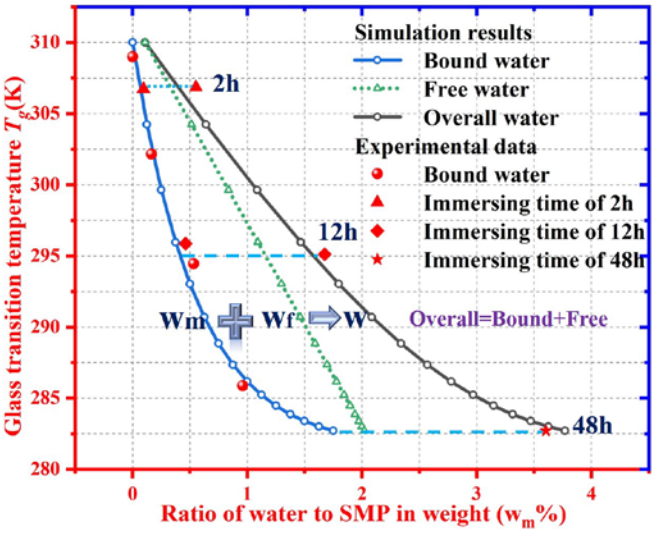
Simulation results
Bound water
Free water
Overall water
Experimental data
Bound water
Immersing time of 2h
Immersing time of 12h
Immersing time of 48h
2h
12h
48h
Wm
Wf
W
Overall=Bound+Free
Glass transition temperature T_g(K)
Ratio of water to SMP in weight (w_m%)
310
305
300
295
290
285
280
0
1
2
3
4

Figure 3.

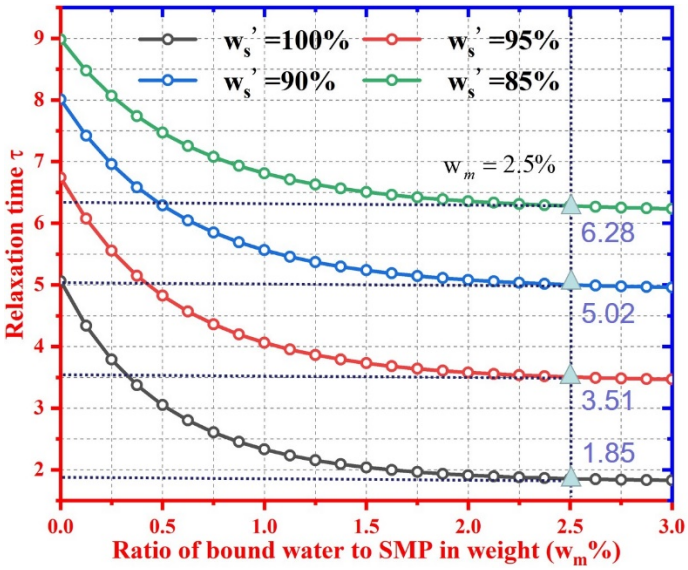
w_s' =100%
w_s' =95%
w_s' =90%
w_s' =85%
w_m = 2.5%
6.28
5.02
3.51
1.85
Relaxation time τ
Ratio of bound water to SMP in weight (w_m%)
0.0
0.5
1.0
1.5
2.0
2.5
3.0
2
3
4
5
6
7
8
9

Figure 4.

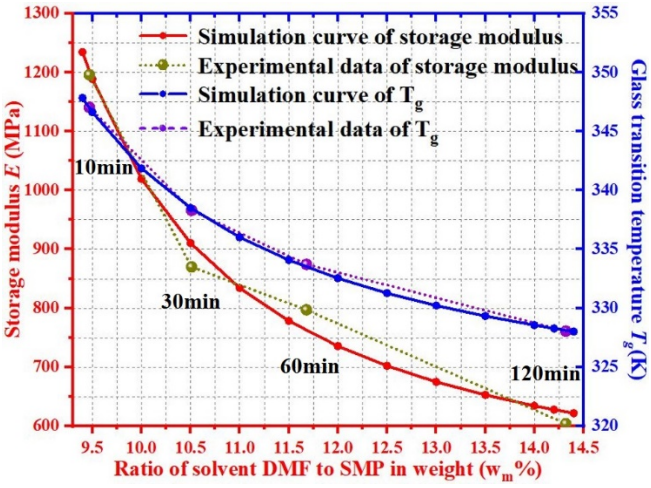
Simulation curve of storage modulus
Experimental data of storage modulus
Simulation curve of T_g
Experimental data of T_g
10min
30min
60min
120min
Storage modulus E (MPa)
Glass transition temperature T_g (K)
Ratio of solvent DMF to SMP in weight (w_m%)
1300
1200
1100
1000
900
800
700
600
355
350
345
340
335
330
325
320
9.5
10.0
10.5
11.0
11.5
12.0
12.5
13.0
13.5
14.0
14.5

Figure 5.

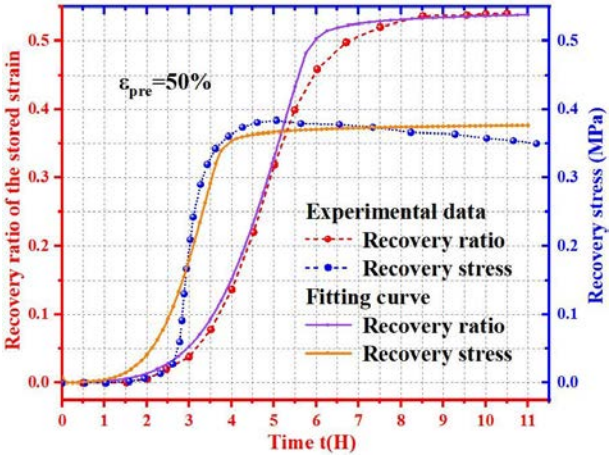
Recovery ratio of the stored strain
Recovery stress (MPa)
Time t(H)
ε_pre=50%
Experimental data
Recovery ratio
Recovery stress
Fitting curve
Recovery ratio
Recovery stress

Figure 6.

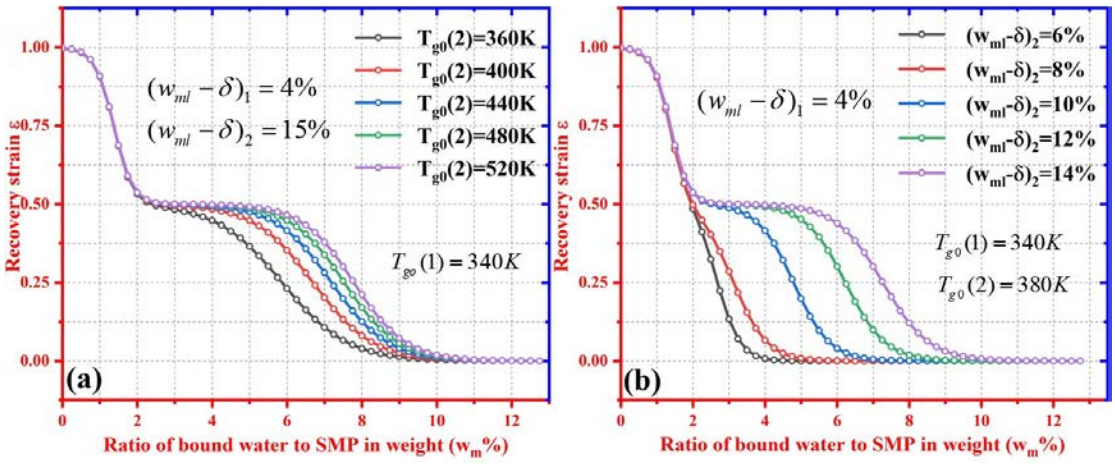
Recovery strain ε
1.00
0.75
0.50
0.25
0.00
$(w_{ml}-\delta)_1 = 4\%$
$(w_{ml}-\delta)_2 = 15\%$
$T_{g0}(2)$=360K
$T_{g0}(2)$=400K
$T_{g0}(2)$=440K
$T_{g0}(2)$=480K
$T_{g0}(2)$=520K
$T_{g0}(1) = 340K$
(a)
0
2
4
6
8
10
12
Ratio of bound water to SMP in weight (w_m%)
Recovery strain ε
$(w_{ml}-\delta)_1 = 4\%$
$(w_{ml}-\delta)_2$=6%
$(w_{ml}-\delta)_2$=8%
$(w_{ml}-\delta)_2$=10%
$(w_{ml}-\delta)_2$=12%
$(w_{ml}-\delta)_2$=14%
$T_{g0}(1) = 340K$
$T_{g0}(2) = 380K$
(b)
Ratio of bound water to SMP in weight (w_m%)

Figure 7.

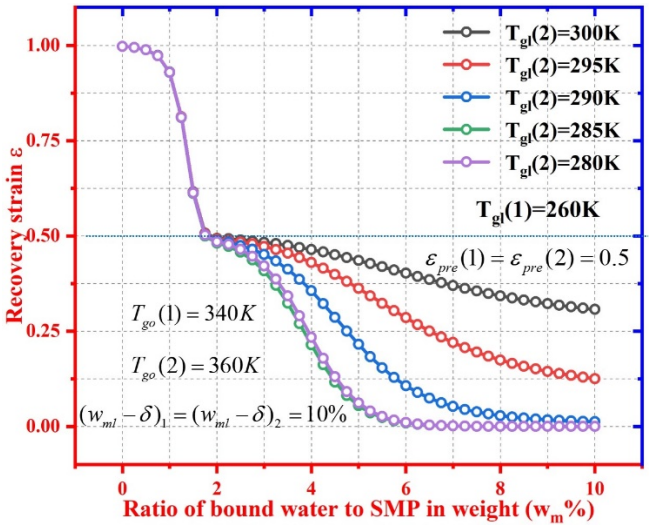
Recovery strain ε
1.00
0.75
0.50
0.25
0.00
0
2
4
6
8
10
Ratio of bound water to SMP in weight (w_m%)
T_gl(2)=300K
T_gl(2)=295K
T_gl(2)=290K
T_gl(2)=285K
T_gl(2)=280K
T_gl(1)=260K
ε_pre(1) = ε_pre(2) = 0.5
T_go(1) = 340K
T_go(2) = 360K
(w_ml − δ)_1 = (w_ml − δ)_2 = 10%

Figure 8.

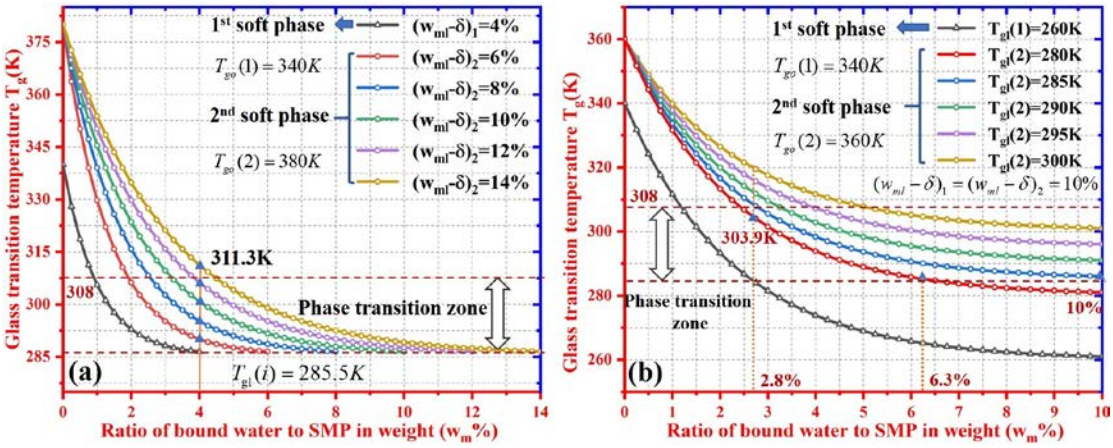
1st soft phase
$T_{go}(1) = 340K$
2nd soft phase
$T_{go}(2) = 380K$
$(w_{ml}-\delta)_1$=4%
$(w_{ml}-\delta)_2$=6%
$(w_{ml}-\delta)_2$=8%
$(w_{ml}-\delta)_2$=10%
$(w_{ml}-\delta)_2$=12%
$(w_{ml}-\delta)_2$=14%
311.3K
308
Phase transition zone
$T_{gl}(i) = 285.5K$
(a)
Glass transition temperature T_g(K)
Ratio of bound water to SMP in weight (w_m%)
1st soft phase
$T_{go}(1) = 340K$
2nd soft phase
$T_{go}(2) = 360K$
$T_{gl}(1)$=260K
$T_{gl}(2)$=280K
$T_{gl}(2)$=285K
$T_{gl}(2)$=290K
$T_{gl}(2)$=295K
$T_{gl}(2)$=300K
$(w_{ml}-\delta)_1 = (w_{ml}-\delta)_2 = 10\%$
308
303.9K
Phase transition zone
10%
2.8%
6.3%
(b)
Glass transition temperature T_g(K)
Ratio of bound water to SMP in weight (w_m%)

Figure 9.

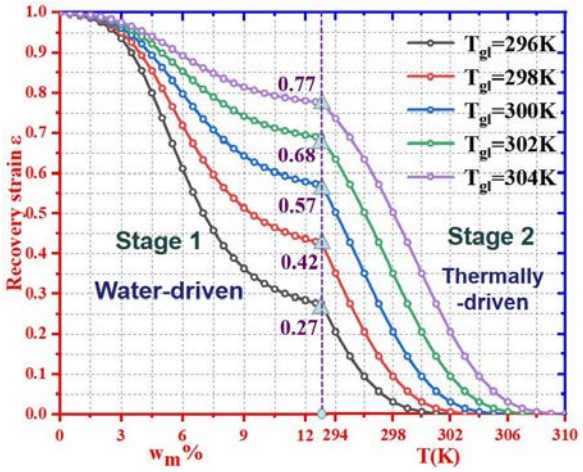
Recovery strain ε
1.0
0.9
0.8
0.7
0.6
0.5
0.4
0.3
0.2
0.1
0.0
0
3
6
9
12
294
298
302
306
310
w_m%
T(K)
T_gl=296K
T_gl=298K
T_gl=300K
T_gl=302K
T_gl=304K
0.77
0.68
0.57
0.42
0.27
Stage 1
Water-driven
Stage 2
Thermally
-driven

Figure 10.